Crystallization and Melting of a Polyethylene Copolymer: *In Situ* Observation by Atomic Force Microscopy

Francis M. Mirabella

Lyondell Chemical Company, Cincinnati, Ohio 45249

Received 29 June 2007; accepted 22 October 2007
DOI 10.1002/app.27739
Published online 18 January 2008 in Wiley InterScience (www.interscience.wiley.com).

ABSTRACT: The isothermal crystallization and subsequent melting of a narrow composition distribution polyethylene (PE) copolymer (containing a few mole percent of an α-olefin) was observed by hot-stage atomic force microscopy (AFM). The observations revealed that a thicker lamellae population formed first, followed by a thinner population. This indicated that the crystallization process occurred in two sequential steps. Initially, a single population of uniform lamellar thickness appeared rapidly and progressively occupied the surface. These skeletal lamellae typically ranged in thickness from about 10–15 nm. Progressively, upon isothermal storage, a second, bridging population of lamellae filled in between this initial skeletal population. This second population was thinner with thicknesses of about 4–6 nm. Upon heating, the second, thinner, bridging population of lamellae melted first, leaving the initial, skeletal population, which melted at higher temperatures. These results indicate that PE copolymers crystallize in a stepwise fashion; this was envisioned to begin with a first step in which the thickest lamellae crystallize from the folding of the longest ethylene sequences, followed by a second step in which shorter sequences, constrained between thicker lamellae, crystallize into a population of thinner crystals. The melting of this presumed bimodal population of crystal thicknesses would produce a broad and bimodal endotherm; the bimodal melting endotherm was observed by differential scanning calorimetry. Furthermore, the lamellar thickness dimensions measured by AFM were in approximately the same range as those calculated from the melting endotherm by means of Gibbs–Thompson theory. © 2008 Wiley Periodicals, Inc. J Appl Polym Sci 108: 987–994, 2008

Key words: crystal structures; crystallization; lamellar; melt; polyethylene (PE)

INTRODUCTION

In a previous article, an *in situ* atomic force microscopy (AFM) study of the crystallization of a polyethylene (PE) copolymer (containing a few mole percent of an α-olefin) narrow copolymer composition distribution (CCD) was reported.[1] It was argued that PE copolymers crystallize in a stepwise fashion, envisioned to begin with a first step in which the thickest lamellae crystallize from the folding of the longest ethylene sequences, followed by a second step in which shorter sequences, constrained between thicker lamellae, crystallize into a population of thinner crystals. The melting of this presumed bimodal population of crystal thicknesses would produce a broad and multimodal endotherm upon melting. However, the interpretation of Stobl and coworkers[1,2] of the temporal sequence during the crystallization of the same type of copolymer was different. The stagewise model proposed by Strobl envisions crystals attaining a variable degree of perfection, i.e. inner stability, and, therefore, variable melting temperature. However, in Strobl's scheme, this is not associated with variability in crystal thickness. Instead, crystals with the same thickness melt at different temperatures, depending on their degree of inner stability. The aim of this study was to observe the crystallization and melting of a PE copolymer by means of *in situ* AFM with a hot stage. In this way, it was anticipated that the nature of the crystallization would be evident and that the question of the variability or constancy of the lamellar thickness would be addressed.

Correspondence to: F. Mirabella, Mirabella Practical Consulting Solutions, Inc., 6948 Hummingbird Drive, Mason, OH 45040 (franmirabella@gmail.com).

Journal of Applied Polymer Science, Vol. 108, 987–994 (2008)

EXPERIMENTAL

Materials

The polymer used in this study was a commercial metallocene-catalyst ultra-low-density polyethylene (M-ULDPE) [3.84 mol %1-butene (18.5 ethyl branches/1000 total C atoms), density = 0.910 g/cc, weight-average molecular weight (M_w) = 108,000, M_w/number-average molecular weight = 2.2].

AFM

AFM was performed on a Veeco (Santa Barbara, CA) multimode scanning probe equipped with a sample heating module capable of heating to 250°C with a temperature accuracy of 3% and a precision of ±0.25°C. The probe was heated to maintain tempera-

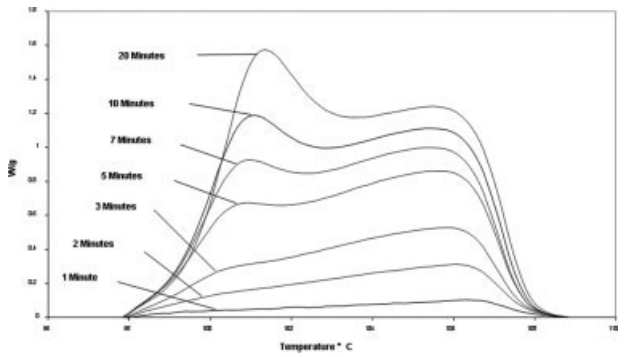

Figure 1 Overlay plot of the endotherms obtained after isothermal crystallizations for various times for M-ULDPE (18.5 ethyl Br/1000 total C, 3.84 mol % 1-butene, T_c = 98.0°C). The heating rate was 10°C/min.

ture equilibrium between the sample stage and probe tip by the application of a specified voltage to the probe. The AFM was operated in tapping mode with silicon probes from μMasch Ultrasharp (Portland, OR) with a resonance frequency of about 300 KHz and a spring constant of about 45 N/m. The probe radius of curvature was about 5 nm. Scanning at 3 Hz required 1.4 min to capture an image. Height and phase contrast images were acquired simultaneously. One micrometer square images required about 1 min to acquire at scanning rate of 3 Hz. The melt surface was sticky. To overcome adhesion of the probe tip to the melt surface, very hard tapping was used, which resulted very noisy images; amplitude set points of 0.3–1.0 were typical. To maintain engagement to the surface, the AFM step motor was used, where necessary, through crystallization events, during which the specimen was contracting due to densification, and during heating, during which the specimen was expanding. The polymer specimens measured by AFM were all compression-molded as thin films (~ 25 μm), placed on a steel disc 12 mm in diameter and 0.13 mm thick without any adhesive and placed directly on the AFM stage.

Differential scanning calorimetry (DSC)

The thermal analysis was done on a PerkinElmer DSC-4 (Waltham, MA) equipped with MC2 thermal analysis software under nitrogen. Indium metal was used as a calibration standard. Sample sizes of about 4 mg were used. The temperature was increased to 150°C, held 3 min, and then rapidly reduced to the isothermal crystallization temperatures (T_c). Melting endotherms were recorded immediately after the respective isothermal crystallization time.

RESULTS AND DISCUSSION

In previous studies, the nature of the crystallization of PE copolymers have been inferred from isothermal crystallization, followed by melting.[1] Evidence of the crystalline structure of such a PE copolymer may be observed in Figure 1, which shows the bimodal melting endotherm of M-ULDPE in Table I (18.5 ethyl Br/1000 total C, T_c = 98.0°C), recorded directly after isothermal crystallization for specified times. The interpretation of this melting endotherm put forward previously[1] was that the longest sequences are envisioned to form the initial thicker, higher T_m lamellae population in an initial crystallization step. Subsequently, the constrained sequences of intermediate length form a thinner, lower melting temperature crystal thickness population, which may be lamellar or possibly fringed micellar. On the contrary, Strobl's scheme envisions that the broad and multimodal melting endotherm is not associated with variability in crystal thickness. Instead, crystals with the same thickness melt at different temperatures, depending on their degree of inner stability.[1,2]

The crystal (lamellar) thickness distribution of the copolymer shown in Figure 1 was calculated from Gibbs–Thompson (G–T) theory[3] and is shown in Figure 2. The thickness distribution was bimodal with a larger crystal thickness peak at about 6.7 nm and a smaller crystal thickness peak at about 7.7 nm. Also, the overall range of crystal thickness shown in Figure 2 was only about 1–1.5 nm.

The ethylene sequence length distribution of M-ULDPE was calculated from eq. (1) and is shown in Figure 3:

$$W_n^o = \left(\frac{n}{2 - X_e}\right)(1-p)^2 p^n \qquad (1)$$

where W_n^o is the probability density, n is the number of ethylene units in the sequence, X_e is the molar

TABLE I
Thermal and Crystal Thickness Data on Narrow Copolymer Composition Distribution Polymers

Sample	T_c (°C)	T_m (°C)	ΔH (J/g)	X_c[a]	DSC (*lc* nm) thickness range[b]	SAXS (*lc* nm)[c]	SAXS (L Å) long period
M-ULDPE	98.0	106.6	95.6	0.332	6.3–8.2	4.7	143

[a] $X_c = \Delta H/288$ J/g.
[b] Lamellar thickness distribution was determined from the DSC endotherm by G–T theory calculations.[3]
[c] Average lamellar thickness was determined by SAXS: $L(X_c) = lc$.
ΔH, enthalpy of fusion; X_c, fraction crystallinity; L, long period; lc, average lamellar thickness.

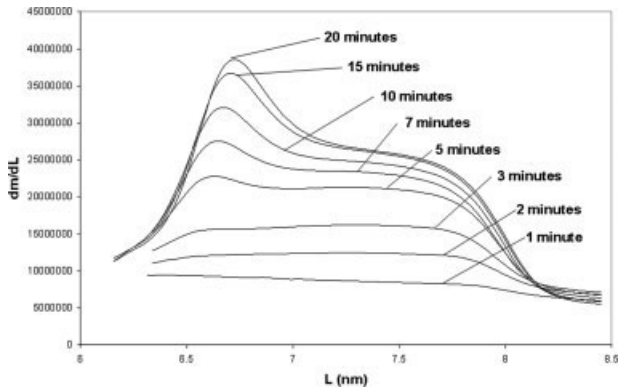

Figure 2 Overlay plot of the lamellar thickness distributions of M-ULDPE after isothermal crystallizations for various times (18.5 ethyl Br/1000 total C, 3.84 mol % 1-butene).

fraction of ethylene in the copolymer, and p is the probability of choosing an ethylene unit that is part of a sequence of ethylene units that is n in length. The distribution shown in Figure 3 was normalized to unit area.

The presumed crystallization sequence is depicted in the two-dimensional schematic in Figure 4. A logical question arises because the ethylene sequence length distribution (e.g., Fig. 3) was unimodal; that is, why was the melting endotherm and, thus, the crystal thickness distribution bimodal? We believe the two-step nature of the crystallization depicted in Figure 4 accounted for this separation into two distinct crystal thickness populations and, therefore, a bimodal thickness distribution. To probe the question of the thickness distribution in an isothermally crystallized copolymer, the crystallization and subsequent melting of the M-ULDPE copolymer were directly observed by hot-stage AFM. AFM phase contrast images are presented to demonstrate the sequential crystallization and subsequent melting of

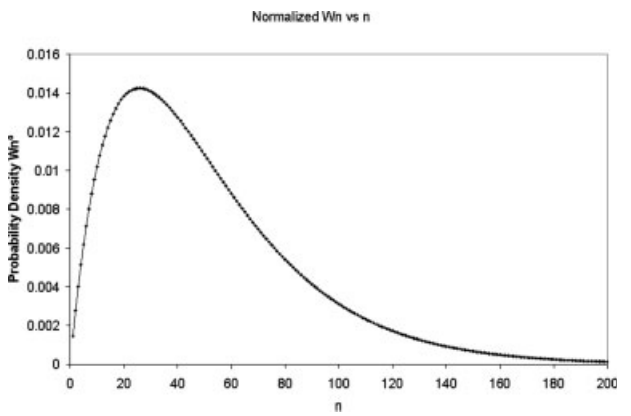

Figure 3 Ethylene sequence length W_n^o function for M-ULDPE (18.5 ethyl Br/1000 total C, 3.84 mol % 1-butene).

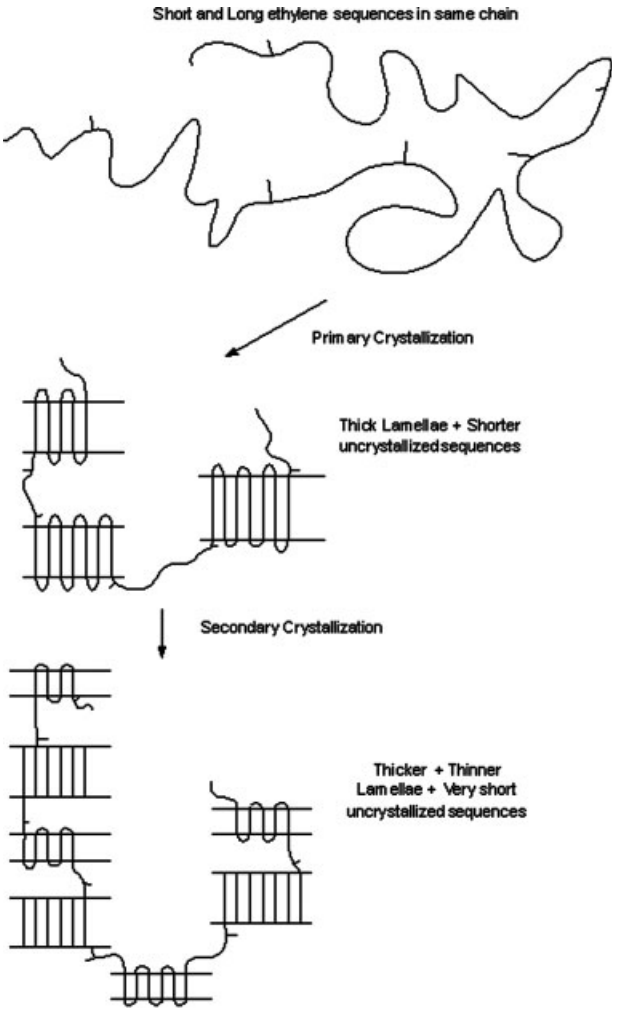

Figure 4 Schematic diagram depicting the sequence of events in the crystallization of the PE copolymer with a broad range of ethylene sequence lengths.

the copolymer. The advantage of this AFM study over that reported previously[1] was that the type of probe used in this study was much sharper, with about half of the radius of curvature, than the probe type used in the previous study.

Figure 5 shows the phase contrast AFM micrograph of the featureless melt of M-ULDPE at 125°C. The temperature was rapidly decreased to an isothermal T_c of 98°C (storage times were the total times of storage in the sequence described). Figure 6 shows the crystallization beginning, as manifest by thin, short lamellar crystals. These crystals lengthened and formed a skeletal structure upon storage for succeeding times of 1.4 and 2.8 m, as shown in Figures 7 and 8, respectively. At 4.2 m of storage, thinner lamellae were observed, bridging the thicker skeletal lamellae and forming a network structure, as shown in Figure 9. This structure of longer, thicker, skeletal lamellae with shorter, thinner, bridging lamellae persisted as time elapsed for succeeding

Figure 5 AFM phase contrast image of M-ULDPE containing 3.8 mol % butene [18.5 ethyl Br/1000 total C (NMR)] at 102°C [cooling (from 125°C)]. The image was 0.5 × 0.5 μm. [Color figure can be viewed in the online issue, which is available at www.interscience.wiley.com.]

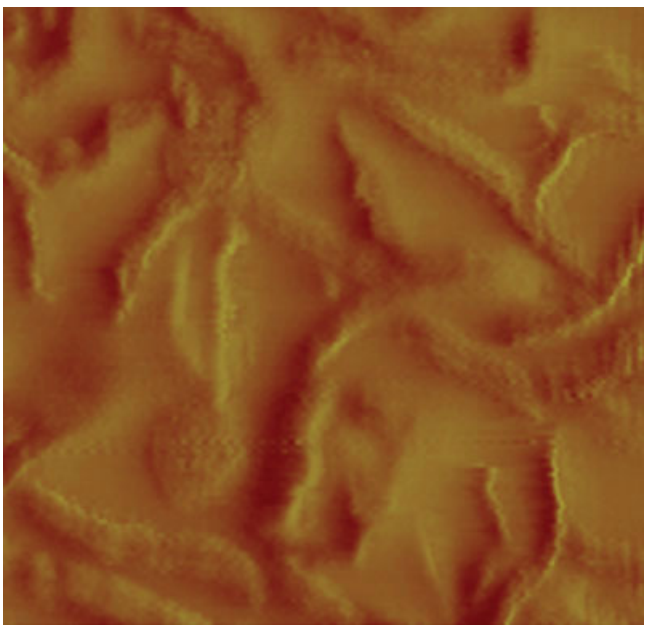

Figure 7 AFM phase contrast image of M-ULDPE at 98°C (cooling; 1.4 min). The image was 0.5 × 0.5 μm. [Color figure can be viewed in the online issue, which is available at www.interscience.wiley.com.]

times of 5.6, 7.0, and 8.4 m, as shown in Figures 10–12, respectively.

The interpretation of the sequence shown in Figures 5–12 is as follows. Initially, a single population of uniform lamellar thickness appeared rapidly and progressively occupied the surface. These skeletal lamellae typically ranged in thickness from about 10 to 15 nm. Progressively, upon isothermal storage, a second, bridging population of lamellae filled in between this initial skeletal population. This second population was thinner with thicknesses of about

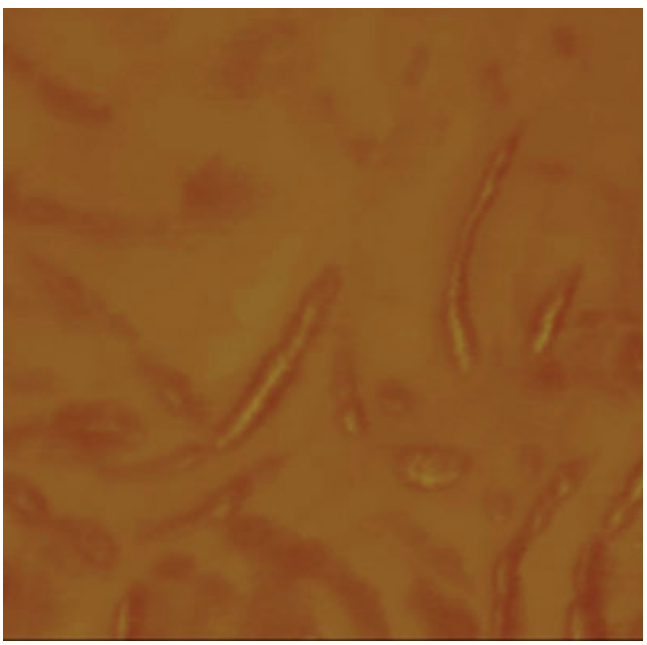

Figure 6 AFM phase contrast image of M-ULDPE at 98°C (cooling; 0 min). The image was 0.5 × 0.5 μm. [Color figure can be viewed in the online issue, which is available at www.interscience.wiley.com.]

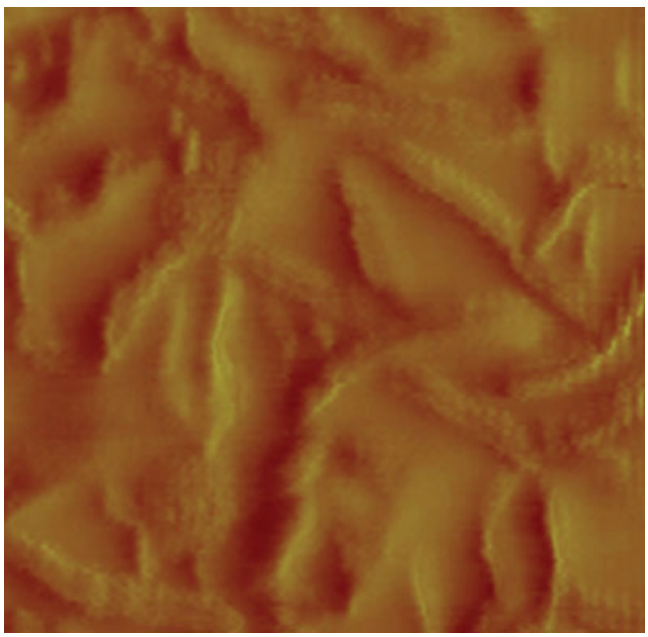

Figure 8 AFM phase contrast image of M-ULDPE at 98°C (isothermal; 2.8 min). The image was 0.5 × 0.5 μm. [Color figure can be viewed in the online issue, which is available at www.interscience.wiley.com.]

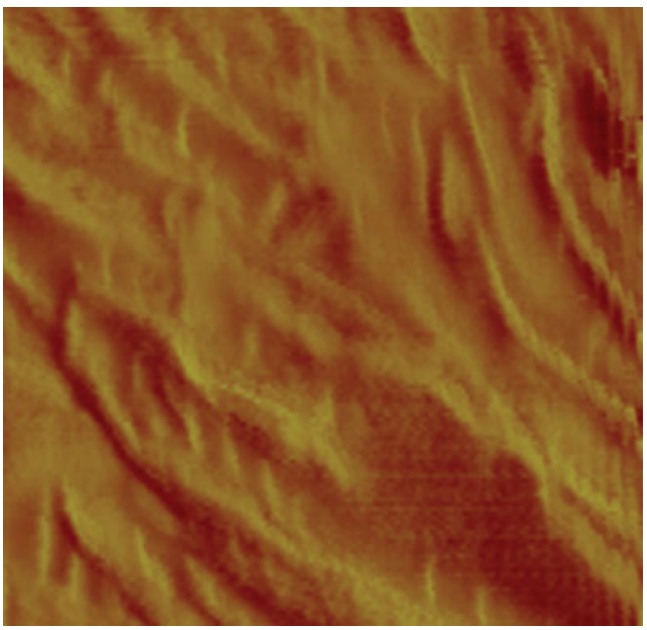

Figure 9 AFM phase contrast image of M-ULDPE at 98°C (isothermal; 4.2 min). The image was 0.5 × 0.5 μm. [Color figure can be viewed in the online issue, which is available at www.interscience.wiley.com.]

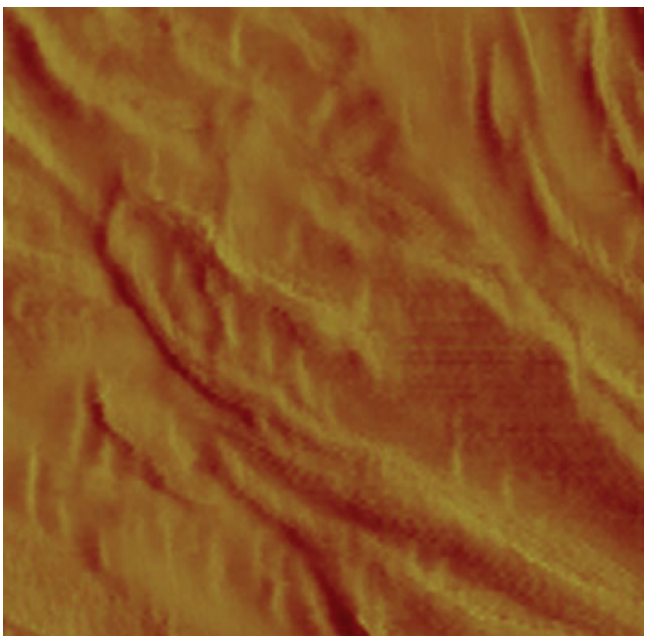

Figure 11 AFM phase contrast image of M-ULDPE at 98°C (isothermal; 7.0 min). The image was 0.5 × 0.5 μm. [Color figure can be viewed in the online issue, which is available at www.interscience.wiley.com.]

4–6 nm. The lamellae preferentially lied with their thickness direction in the surface plane of the melt. This was the lowest energy configuration for the lamellae, which had a fold surface free energy of 90 mJ/m^2 and a lateral surface free energy 11.8 mJ/m^2.[1] The lamellar thickness dimensions measured by AFM were in approximately the same range as those shown in Figure 2 calculated from G–T theory.

Upon heating, the second, thinner, bridging population of lamellae melted first, which left the initial, skeletal population, which melted at higher temperatures. This may be observed in Figures 13–18. The

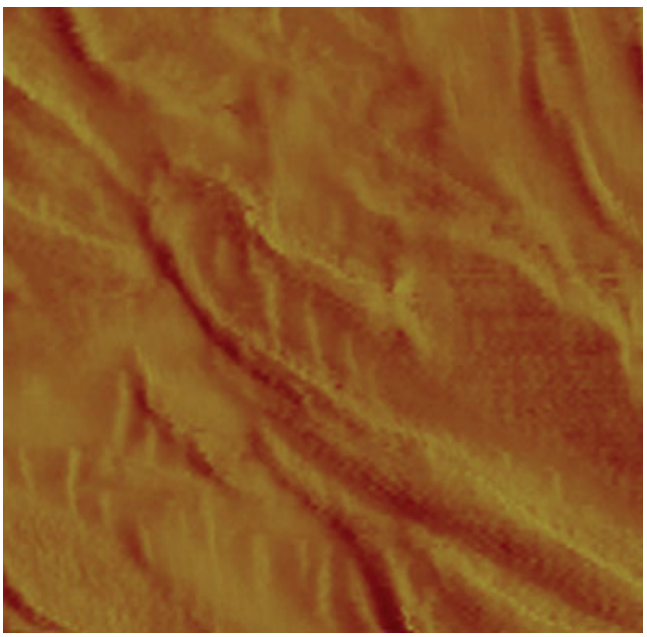

Figure 10 AFM phase contrast image of M-ULDPE at 98°C (isothermal; 5.6 min). The image was 0.5 × 0.5 μm. [Color figure can be viewed in the online issue, which is available at www.interscience.wiley.com.]

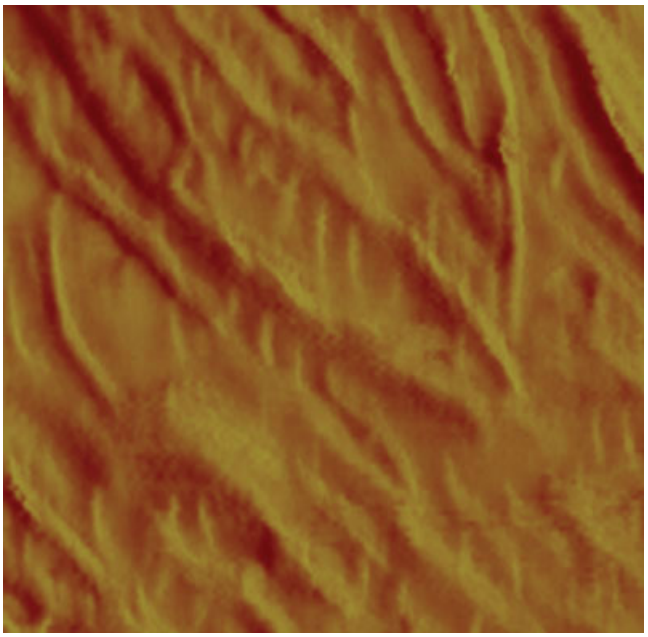

Figure 12 AFM phase contrast image of M-ULDPE at 98°C (isothermal; 8.4 min). The image was 0.5 × 0.5 μm. [Color figure can be viewed in the online issue, which is available at www.interscience.wiley.com.]

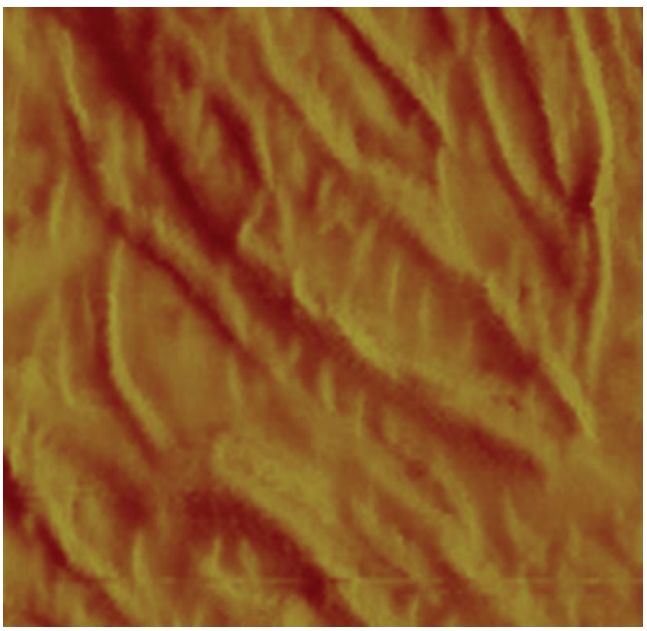

Figure 13 AFM phase contrast image of M-ULDPE at 101°C (heating). The image was 0.5 × 0.5 μm. [Color figure can be viewed in the online issue, which is available at www.interscience.wiley.com.]

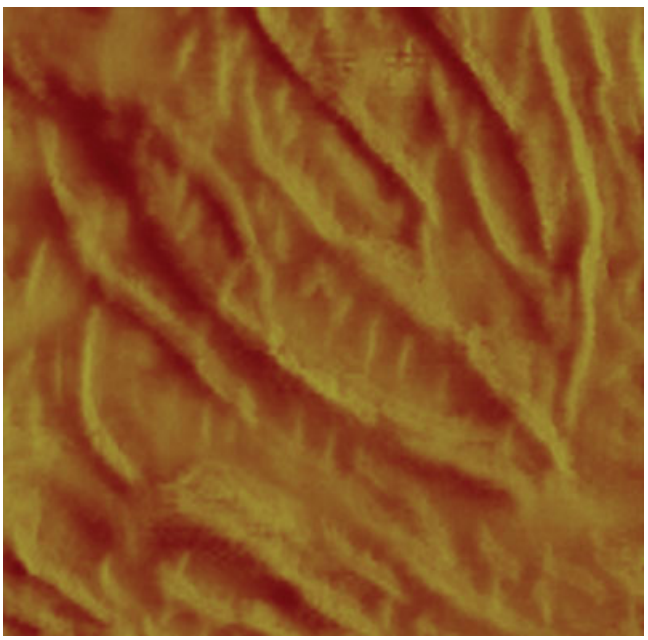

Figure 15 AFM phase contrast image of M-ULDPE at 105°C (heating). The image was 0.5 × 0.5 μm. [Color figure can be viewed in the online issue, which is available at www.interscience.wiley.com.]

temperature was increased progressively, as shown in Figures 13–15, to 101, 103, and 105°C, respectively. The thinner, bridging lamellae did not melt up to 105°C, as shown in Figures 13–15. Upon heating to 107°C, the thinner, bridging lamellae melted, but the skeletal lamellae did not melt, as shown in Figure 16. After further heating to 109°C, the skeletal lamellae did not melt, as shown in Figure 17. At this point in the experiment, further heating resulted in a loss of engagement to the surface. Imminent loss of engagement was evidenced by the degrading images shown in Figures 16 and 17. In other experiments

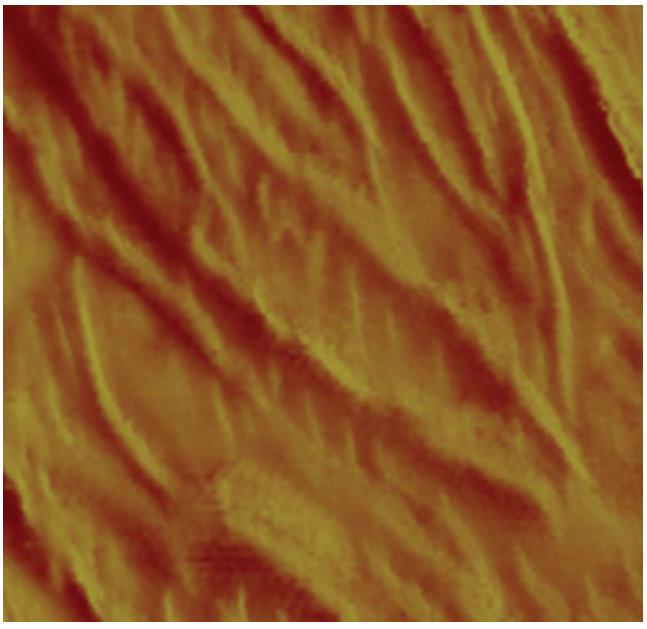

Figure 14 AFM phase contrast image of M-ULDPE at 103°C (heating). The image was 0.5 × 0.5 μm. [Color figure can be viewed in the online issue, which is available at www.interscience.wiley.com.]

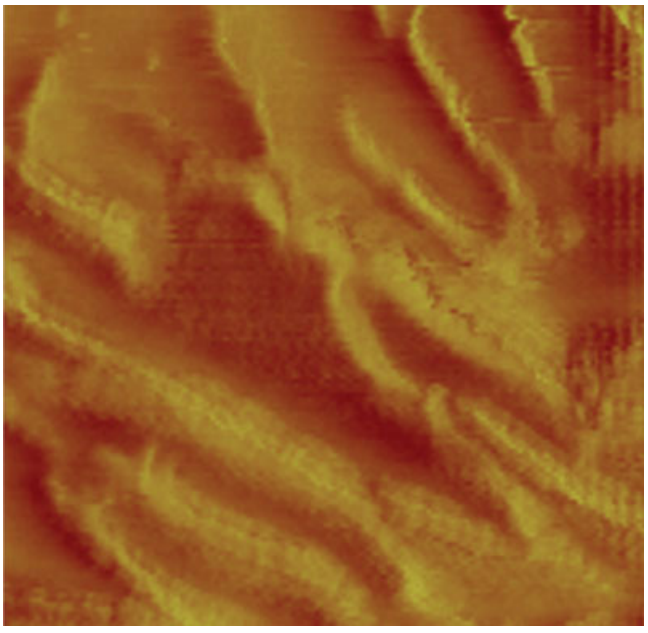

Figure 16 AFM phase contrast image of M-ULDPE at 107°C (heating). The image was 0.5 × 0.5 μm. [Color figure can be viewed in the online issue, which is available at www.interscience.wiley.com.]

(not shown), the skeletal lamellae melted at temperatures above 110°C.

The temporal sequence of crystallization observed in the AFM could be correlated with the temporal sequence of isothermal crystallization at 98°C observed in the DSC experiments and shown in Figure 1. Upon isothermal storage at 98°C for about 3 m in the AFM observations, a thicker population of lamellae crystallized (Fig. 8), which was consistent with the higher melting crystals arising first over about 3 m, as shown in Figure 1. The thinner lamellae population was first observed at 4.2 m in the AFM images (Fig. 9), and this was consistent with the increasing preponderance of the lower melting temperature crystals observed between 3 and 5 m, shown in Figure 1. The lower melting temperature crystals went on increasing in preponderance from 5 to 20 m, as shown in Figure 1, and also persisted in the AFM experiments from 4.2 to 8.4 m of isothermal storage (Figs. 10–12).

The sequence of melting as a function of temperature observed independently by AFM and DSC could also be correlated. The thinner lamellae persisted in the AFM experiment from 101 to 105°C (Figs. 13–15) and melted between 105 and 107°C (Fig. 16), and this was approximately consistent with the data shown in Figure 1, in which the lower melting temperature crystals melted between about 103 and 105°C. In other experiments (not shown), the skeletal lamellae melted at temperatures above 110°C, which was consistent with the data shown in Figure 1. The lack of precision in the comparison of the AFM and DSC experiments was probably due to the large temperature jumps used in the AFM experiment.

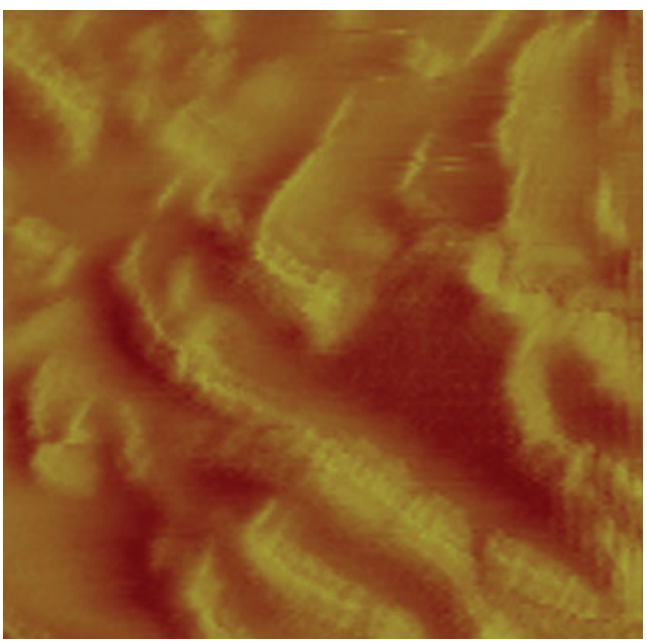

Figure 17 AFM phase contrast image of M-ULDPE at 109°C (heating). The image was 0.5 × 0.5 μm. [Color figure can be viewed in the online issue, which is available at www.interscience.wiley.com.]

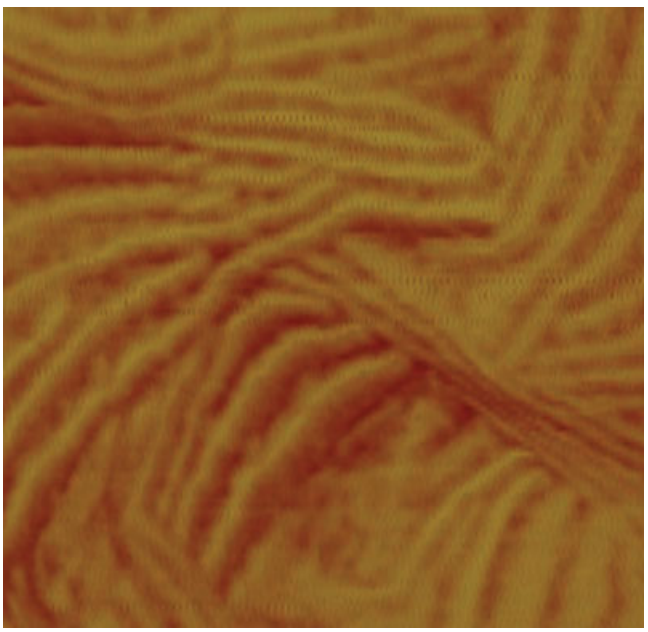

Figure 18 AFM phase contrast image of M-ULDPE at room temperature. The image was 0.5 × 0.5 μm. [Color figure can be viewed in the online issue, which is available at www.interscience.wiley.com.]

The second, thinner, bridging population of lamellae was observed to be oriented at roughly right angles to the initial, thicker, skeletal lamellae. As explained previously, the thinner lamellae population was presumed to form from shorter ethylene sequences, which were constrained between already crystallized longer ethylene sequences. This constraint may have disposed the shorter sequences to crystallize at right angles to the thicker lamellae.

Approximately, the same area of the specimen was quenched to room temperature in the AFM experiments. Figure 18 shows the morphology of the room-temperature crystals. The crystalline morphology shown in Figure 18 was composed of long lamellar edges. Some basal planes were partially exposed due to the twisting of the lamellae. Also shown in Figure 18 are some of the structures with longer, thicker lamellae bridged by shorter, thinner lamellae at roughly 90° angles.

CONCLUSIONS

In situ observation by hot-stage AFM of the isothermal crystallization and subsequent melting of a narrow composition distribution PE copolymer revealed that a thicker lamellar thickness population formed first, followed by a thinner population. This indi-

cated that the crystallization process occurred in two sequential steps. Initially, a single population of uniform lamellar thickness appeared rapidly and progressively occupied the surface. These skeletal lamellae typically ranged in thickness from about 10 to 15 nm. Progressively, upon isothermal storage, a second, bridging population of lamellae filled in between this initial skeletal population. This second population was thinner with thicknesses of about 4–6 nm. Upon heating, the second, thinner, bridging population of lamellae melted first, leaving the initial, skeletal population, which melted at higher temperatures. These results indicated that PE copolymers (containing a few molar percentages of an α-olefin) crystallized in a stepwise fashion, envisioned to begin with a first step in which the thickest lamellae crystallized from the folding of the longest ethylene sequences, followed by a second step in which shorter sequences, constrained between thicker lamellae, crystallized into a population of thinner crystals. The melting of this presumed bimodal population of crystal thicknesses would produce a broad and bimodal endotherm. In fact, a bimodal melting endotherm was observed by DSC, which melted over a similar temperature range in the *in situ* AFM experiment. Furthermore, the lamellar thickness dimensions measured by AFM were in approximately the same range as those calculated from the melting endotherm by means of the G–T theory. The second, thinner, bridging population of lamellae was observed to be oriented at roughly right angles to the initial, thicker, skeletal lamellae. We presumed that the thinner lamellae population formed from shorter ethylene sequences, which were constrained between already crystallized longer ethylene sequences. This constraint may have disposed the shorter sequences to crystallize at right angles to the thicker lamellae.

The author gratefully acknowledges the assistance of Douglas McFaddin for the NMR measurements, Brandon Dunphy for the DSC measurements and the preparation of the preparative temperature rising elution fractionation (P-TREF) fractions, and Gregory Beaucage for the small-angle X-ray scattering (SAXS) measurements. The author gratefully acknowledges helpful discussions with Gregory Beaucage and Buckley Crist.

References

1. Mirabella, F. M. J Polym Sci Part B: Polym Phys 2006, 44, 2369.
2. Strobl, G. Eur Phys J 2000, E 3, 165.
3. Crist, B.; Mirabella, F. M. J Polym Sci Part B: Polym Phys 1999, 37, 3131.